Ground- and Excited-State Mapping of Plastocyanin from Resonance Raman Spectra of Isotope-Labeled Proteins

Shoulian Dong and Thomas G. Spiro*

Contribution from the Department of Chemistry, Princeton University, Princeton, New Jersey 08544

Received December 29, 1997

Abstract: Resonance Raman (RR) spectra are reported for recombinant *poplar* plastocyanin, which was isotopically labeled with cysteine-$C_\beta D_2$ and -^{15}N. Abundantly expressed protein and careful low-temperature scanning permitted resolution of an unprecedented number of bands in the 400 cm^{-1} region and determination of their isotope shifts. These shifts confirm extensive mixing of ligand internal coordinates with the Cu−S(Cys) stretching coordinate and also reveal mixing into the mainly Cu−N(His) stretching mode at 267 cm^{-1}. RR scattering is observed for combinations of this mode with all of the ∼400 cm^{-1} modes as well as of the ∼400 cm^{-1} modes with one another. In addition, the isotopic labeling establishes the assignment of higher-frequency RR-enhanced fundamental modes, S−C stretching, methylene twisting and scissoring, and the amide III mode, all of which are localized on cysteine, as well as three imidazole ring modes of histidine. The 1040 cm^{-1} imidazole peak is definitively assigned to the ligating His87 because it shifts cleanly to 1054 cm^{-1} upon brief exposure to D_2O, which is known to permit selective NH/D exchange of the solvent-exposed imidazole ring of His87. Selective enhancement of His87 modes is ascribed to the orientation of the imidazole ring, which allows mixing of imidazole and sulfur π orbitals in the resonant charge-transfer excited states. Support for this mixing is provided by the RR excitation profiles, which reveal a 20-nm red-shift of the scattering maximum for modes localized on histidine, relative to those localized on cysteine. Both coordinate mixing and RR enhancement of internal ligand modes are ascribed to coplanarity of the atoms in the electron-transfer pathways to the remote (Tyr83) site and their alignment with the imidazole ring of the adjacent (His87) site for electron transfer, a geometry that maximizes the electronic coupling along both pathways.

1. Introduction

Plastocyanin (Pcy), a prototypical type 1 copper protein, mediates long-range electron transfer in the photosynthetic system of higher plants and green algae, shuttling electrons from reduced cytochrome b_6f to the photooxidized chlorophyll-containing pigment P700$^+$.[1] In the X-ray crystal structure of oxidized *poplar* plastocyanin,[2] the copper ion is coordinated to the side chains of a cysteine (Cys84) and two histidine (His87 and -37) residues, plus a weakly bound methionine (Met92), arranged in a distorted tetrahedral coordination group (Figure 1). Due to this unusual geometric structure, Pcy, like other type 1 Cu proteins, has intense blue color, which has been ascribed to S_{Cys} to Cu charge-transfer transitions.[3] Detailed studies by Solomon and co-workers[4] have assigned the most intense absorption (600 nm) to S_{Cys} $p_\pi \rightarrow$ Cu $d_{x^2-y^2}$ charge transfer, with some contribution of imidazole π orbitals, and a high energy shoulder (520 nm) to a S_{Cys} pseudo-$\sigma \rightarrow$ Cu $d_{x^2-y^2}$ transition. The Cu-ligand field transitions produce weak bands at lower energy; the one with highest energy (717 nm) is assigned to the Cu d_{xz-yz} to $d_{x^2-y^2}$ transition.

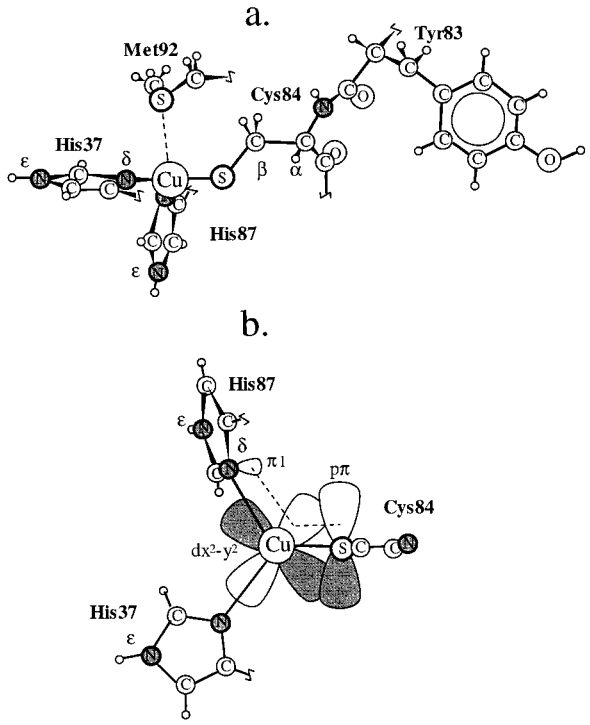

Figure 1. The active site *poplar* Pcy, showing the orientation of ligating side chains, and the extended framework out to the remote Tyr83 site.

Resonance Raman (RR) spectra excited at wavelengths within the 600 nm absorption band are surprisingly complex.[5] Enhancement is expected for Cu-ligand stretching vibrations, which should occur near 250 cm^{-1} for the Cu−N(His) bonds (because

* To whom correspondence should be addressed.

(1) (a) Sykes, A. G. *Struct. Bonding (Berlin)* **1990**, *75*, 175−224. (b) Sykes, A. G. *Adv. Inorg. Chem.* **1991**, *36*, 377−408. (c) Ryden, L. In *Copper Proteins and Copper Enzymes*; Lontie, R., Ed.; CRC Press: Boca Raton, FL, 1984, pp 157−182.

(2) (a) Colman, P. M.; Freeman, H. C.; Guss, J. M.; Murata, M.; Norris, V. A.; Ramshaw, J. A.; Venkatappa, M. P. *Nature (London)*, **1978**, *272*, 319−324. (b) Adman, E. T. *Adv. Protein Chem.* **1991**, *42*, 145−198.

(3) Gray, H. B.; Solomon, E. I. In *Copper Proteins*; Spiro, T. G., Ed.; Wiley: New York, 1981; pp 1−39.

(4) (a) Solomon, E. I.; Baldwin, J.; Lowery, M. D. *Chem. Rev.* **1992**, *92*, 521−524. (b) Solomon, E. I.; Lowery, M. D. *Science* **1993**, *259*, 1575−1581.

S0002-7863(97)04377-1 CCC: $15.00
Published on Web 09/25/1998

of the large effective mass of the imidazole rings[6]), and near 400 cm^{-1} for the Cu−S(Cys) bond (because of the short Cu−S distance, ∼2.1 Å[7]). The former have been assigned to relatively isolated ∼250 cm^{-1} peaks,[6] but numerous peaks are enhanced in the 400 cm^{-1} region. Isotope labeling of Pcy[8] and of azurin,[9,10] using bacterial expression systems, has revealed that the Cu−S(Cys) coordinate mixes strongly with internal ligand coordinates, especially of cysteine, to produce the complex modes in the 400 cm^{-1} region. Progress has been made in modeling this mixing using a chromophore-within-protein computational approach.[11]

The RR spectra are also of interest with respect to the mechanism of electron transfer (ET) in type 1 Cu proteins, because the charge-transfer excited states, whose character determine the RR enhancement pattern, represent virtual steps in the ET pathway.[12] RR intensities have recently been analyzed for Pcy from this point of view.[13] However, there is still much to be determined about the nature of these states, as the present results illustrate. We have labeled Pcy with ^{15}N- and $C_\beta D_2$-containing cysteine and have carried out selective NH/D exchange of the His87 imidazole. The isotope shifts confirm that the ∼400 cm^{-1} vibrations are heavily admixed with cysteine internal coordinates. Surprisingly, they also reveal that the 267 cm^{-1} Cu−N(His) mode likewise has significant cysteine contributions. More importantly, the isotope shifts permit assignments of high-frequency RR bands to internal vibrations of His87 as well as of Cys84. Finally the RR excitation profiles (EP's) are found to distinguish between His87 and Cys84 modes. The EP maximum is red-shifted by 16 nm (450 cm^{-1}) for the His87 modes, indicating that the 600-nm absorption band contains multiple transitions, involving His87 as well as Cys84 donor orbitals. This mixing is attributed to alignment of the imidazole and S(Cys) π orbitals. This alignment extends to the Tyr83 residue adjacent to Cys84, which is the "remote" site of ET from the physiological reductant. The extended alignment, which is expected to maximize the electronic coupling along the ET pathway, accounts for the extensive coordinate mixing in the ground-state vibrations as well as for the vibrational structure of the CT excited states.

2. Experimental Section

Protein Preparation and Selective Labeling. The Pcy was produced by overexpressing the cloned *poplar* gene Pcy/pET3a in *Escherichia coli*, X90 (DE3), as reported previously.[8] Uniform ^{15}N labeling was achieved by growing the same *E. coli* in M9 minimal medium with $^{15}NH_4Cl$ supplied as the sole nitrogen source.

To selectively label Cys of Pcy, the gene construction Pcy/pET3a was transformed into the *E. coli* auxotroph JM15 (DE3)/pLys (*cysE50, trf-8*) (a gift from Professor John L. Markley (University of Wisconsin, Madison)) using the standard protocol.[14] Transformants containing the Pcy/pET3a plasmid were selected by their antibiotic resistance to ampicillin and chloramphenicol. The protein was then expressed in M9 minimal medium supplemented with 1 mM cupric citrate, the 20 amino acids (Sigma) and five nucleotides (A, C, G, T, and U) according to the literature.[15] The cysteine was supplied as DL-3, 3-D_2-Cys (98%) or l-^{15}N-Cys (95−99%) (Cambridge Isotope Laboratories). One liter of medium was inoculated with a colony from an agar LB plate and incubated at 28 °C in a shaker to $OD_{600} = 0.6-1.0$ before being induced with 100 mg of IPTG. After further incubation for 6 h, the bacteria were pelleted by centrifugation at 4 °C. Proteins were released from the cells by three freeze/thaw cycles[16] and dissolved in 15 mL of 0.5% $MgCl_2$ solution containing 1 mM cupric citrate. The crude protein solution was separated from the cell debris by centrifugation and dialyzed exhaustively against 0.5% $MgCl_2$ solution before it was purified to an absorption ratio A_{276}/A_{597} of 1.1−1.2[17] by HPLC. The concentrated purified plastocyanin was divided into aliquots and stored at −20 °C and then exchanged with appropriate buffers by ultrafiltration (Amicon centriprep) just prior to spectroscopic measurements. The final protein concentration was determined from the absorptivity at 597 nm ($\epsilon_{597} = 4500\ M^{-1}\ cm^{-1}$).[1a]

H/D exchange experiments were carried out in two ways to achieve different extents of exchange. The ϵNH on His87 was selectively exchanged[18] with D by dissolving lyophilized protein in 20 mM bis-Tris buffer (pH 6.0) and by quenching the resulting mixture in D_2O in a liquid nitrogen dewar.[19] More extensive H/D exchange was achieved by incubation in a sealed vial (4 °C for 5 days) after 50-fold dilution of protein in D_2O (pD 6.0, 20 mM bis-Tris buffer with 150 mM NaCl) followed by reconcentration by ultrafiltration.

Resonance Raman Spectroscopy. RR spectra were collected in backscattering geometry (∼135°) from frozen drops of protein solution (20 μL, 3−5 mM) on a liquid N_2 coldfinger.[19] This technique minimizes sample requirements and produces sharpened RR spectra. Signals were collected with a triple monochromator (Spex 1877, 3 cm^{-1} spectral slit width) with an intensified diode array detector (Princeton Instruments). Excitation was provided at several Ar^+ and Kr^+ laser wavelengths. For accurate comparison of spectra, the samples were loaded side by side. Absolute peak positions (±1 cm^{-1} estimated accuracy) were calibrated with the known spectra of indene and *N,N*-dimethylformide. For excitation profiles, deconvoluted peak areas were measured relative to the ice peak at 225 cm^{-1} (low-frequency region, 267−440 cm^{-1}) or to the 990 cm^{-1} peak of SO_4^{2-} internal standard (high freqency region). The intensities were converted to absolute cross sections using $(d\sigma/d\Omega)_p = I_p/I_{SO4^{2-}} \times (d\sigma/d\Omega)_{SO4^{2-}}$ where $(d\sigma/d\Omega)_p$ is the cross section of a protein band, $(d\sigma/d\Omega)_{SO4^{2-}}$ is the cross section[20] for SO_4^{2-} corrected for the ν^4 dependence[20b] and $I_p/I_{SO4^{2-}}$ is the intensity ratio of the protein band and the SO_4^{2-} band. The ice peak was normalized against the sulfate peak.

(5) (a) Woodruff, W. H.; Dyer, R. B.; Schoonover, R. B. In *Biological Application of Raman Spectroscopy*; Spiro, T. G., Ed.; Wiley: New York, 1988; Vol. III, pp 413−438. (b) Sanders-Loehr, J. In *Bioinorganic Chemistry of Copper*; Kalin, K. D., Tyeklar, Z., Eds.; Chapman Hall: New York, 1993, pp 51−63. (c) Blair, D. F.; Campbell, G. H.; Schoonover, J. R.; Chan, S. I.; Gray, H. B.; Malmstrom, B. G.; Pecht, I.; Swanson, B. I.; Woodruff, W. H.; Cho, W. K.; English, A. M.; Fry, H. A.; Lum, V.; and Notron, K. A. *J. Am. Chem. Soc.* **1985**, *107*, 5755−5766.

(6) Nestor, L.; Larrabee, J.; Wooley, A. G.; Reinhammar, B.; Spiro, T. G. *Biochemistry* **1984**, *23*, 1084−1093.

(7) Guss, J. M.; Bartunk, H. D.; Freeman, H. C. *Acta Crystallogr.* **1992**, *B48*, 790−811.

(8) Qiu, D.; Dong, S.; Ybe, J. A.; Hecht, M. H.; Spiro, T. G. *J. Am. Chem. Soc.* **1995**, *117*, 6443−6446.

(9) (a) Dave, B. C.; Germanas, J. P. and Czernuszewicz, R. S. *J. Am. Chem. Soc.* **1993**, *115*, 12175−12176. (b) Czernuszewicz, R. S., private communication.

(10) (a) Andrew, C. R.; Han, J.; den Blaauwen, T.; van Pouderoyen, G.; Vijgenboom, E.; Canters, G. W.; Loehr, T. M.; Sanders-Loehr, J. *J. Biol. Inorg. Chem.* **1997**, *2*, 98−107. (b) Andrew, C. R.; Yoem, H.; Valentine, J. S.; Karlsson, B. G.; Bonander, N.; van Prouderoyen, G.; Canters, G. W.; Loehr, T. M.; Sanders-Loehr, J. *J. Am. Chem. Soc.* **1994**, *116*, 11489−11498.

(11) Qiu, D.; Dasgupta, S.; Goddard, W. A., III.; Spiro, T. G., submitted.

(12) Myers, A. B. *Chem. Rev.* **1996**, *96*, 911−926.

(13) Fraga, E.; Webb, M. A.; Loppnow, G. R. *J. Phys. Chem.* **1996**, *100*, 3278−3287.

(14) Manitis, T.; Fritsh, E. F.; Sambrook, J. *Molecular Cloning, A Laboratory Manual*; Cold Spring Harbor Laboratory: Cold Spring Harbor, New York, 1982.

(15) Cheng, H.; Westler, W. M.; Xia, B.; Oh, B. H.; Markley, J. L. *Arch. Biochem. Biophys.* **1995**, *316*, 619−635.

(16) Ybe, J. A.; Hecht, M. H. *Protein Expression Purif.* **1994,** *5*, 317−323. Johnson, B. H.; Hecht, M. H. *Biotechnology* **1994**, *12*, 1357−1360.

(17) (a) Katoh, S.; Shiratori, I.; Takamiya, A. *J. Biochem.* **1962**, *51*, 32−40. (b) Nordling, M.; Olausso, T.; Lundberg, L. G. *FEBS Lett.* **1990**, *276*, 98−102.

(18) (a) Markley, J. L. *Acc. Chem. Res.* **1975**, *8*, 70−80. (b) Markley, J. L.; Ulrich, E. L.; Berg, S. P.; Krogmann, D. W. *Biochemistry* **1975**, *14*, 4428−4433.

(19) Czernuszewicz, R. S.; Johnson, M. K. *Appl. Spectrosc.* **1983**, *37*, 297−298.

(20) (a) Shomacker, K. T.; Champion, P. M. *J. Chem. Phys.* **1989**, *90*, 5982−5993. (b) Dudik, J. M.; Johnson, C. R.; Asher, S. A. *J. Chem. Phys.* **1982**, *82*, 1732−1740.

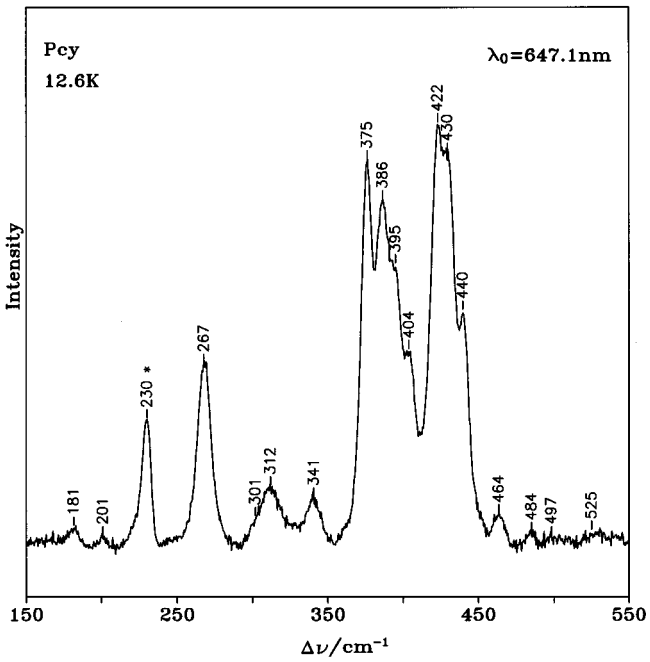

Figure 2. RR spectrum of 1.5 mM Pcy on scanning spectrometer. The sample was held in a copper block which was connected to a Displex cryotip. Temperature was maintained at 12.6 K during the experiment. Spectral conditions: laser, $\lambda = 647.1$ nm (140 mW); spectral slit width = 3 cm^{-1}; scan speed = 0.5 cm^{-1}/s; 180° backscattering geometry; 12 scans averaged together. Solution conditions: pH = 6.0, 20 mM bis-Tris buffer with 150 mM NaCl. The * denotes a plasma line overlapped with the 227 cm^{-1} ice peak.

To precisely determine positions of the RR peaks around 400 cm^{-1}, we collected the data with a scanning double monochromator (Spex1404, with a RCA31034A photomultiplier tube detector) at 3 cm^{-1} slit width. Eight to twelve scans were accumulated and averaged for each spectrum. The spectrum of carbon tetrachloride was collected before and after the protein spectra. Band positions were determined by deconvolution with Labcalc (Galactic Industries Corp.) using isotope-independent bandwidths. The precision is estimated from repeated experiments to be better than ±0.2 cm^{-1}.

3. Results

3.1. Low-Frequency Fundamentals at 250−470 cm^{-1}. Extensive Coordinate Mixing. With the large quantities of protein available from the overexpression system,[16] we were able to obtain Pcy spectra of unprecedented quality. They are consistent with published spectra in the 240−500 cm^{-1} range[5c,6,8,21] but reveal additional weak features at 181, 201, 312, 341, 464, 484, 497, and 525 cm^{-1} (Figure 2). In the crowded 350−450 cm^{-1} region, the number of peaks has been variously reported as three or five, but the high-resolution data obtained with the scanning double monochromator require seven peaks for an accurate fit to the spectrum (Figure 3). To determine isotope shifts (Figure 4 and Table 1), these seven peaks were fit to each spectrum using isotope-independent bandwidths.

As with previously measured isotopes,[8] the shifts are found to be spread throughout the low-frequency modes, and provide additional evidence for extensive mixing of internal ligand coordinates with the metal−ligand stretching coordinates.[8,11] Interestingly, even the 267 cm^{-1} band, long assigned to Cu−N(His) stretching,[6] shifts appreciably when the Cys ligand is labeled at the C_β and amide N atoms, establishing that internal

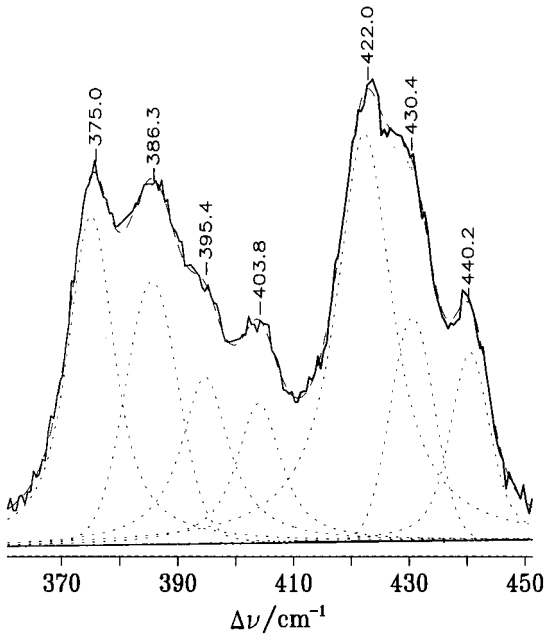

Figure 3. Deconvolution of the RR bands around 400 cm^{-1} for N. A. Pcy at 77 K. Experimental conditions are the same as in Figure 2. Solid line denotes actual spectrum; dashed line denotes curvefit; dotted line denotes subpeaks.

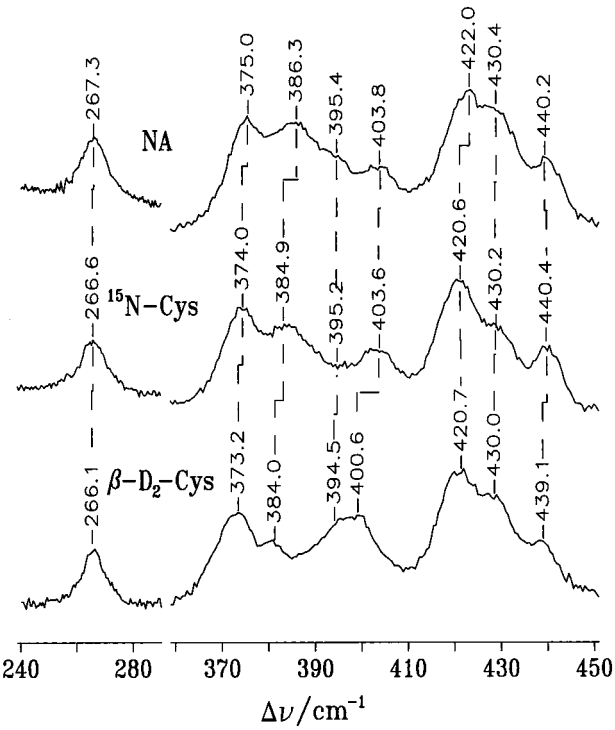

Figure 4. RR spectra of N. A. and ^{15}N-Cys and β-D_2-Cys labeled Pcy's collected on the double monochromator. The samples were maintained at 77 K with a liquid nitrogen dewar. The samples were exchanged to pH 5.5 20 mM piperazine buffer containing 300 mM NaCl with Amicon centriprep. The spectral conditions are the same as in Figure 2.

cysteine coordinates are also mixed into this mode. Moreover, the band shifts 1 cm^{-1} when Pcy is quenched in D_2O, resulting in selective NH/D exchange for the His87 imidazole ring,[18] but it shifts 3 cm^{-1} after 5 days of incubation in D_2O. Under these conditions there is no NH/D exchange into the other imidazole ligand, His37 (nor is there any CH/D exchange in either

(21) Woodruff, W. H.; Norton, K. A.; Swanson, B. I.; Fry, H. A. *Proc. Natl. Acad. Sci. U.S.A.* **1984**, *81*, 1263−1267.

Table 1. Isotopic Shifts and Assignments for the Fundamental Vibrations of Plastocyanin

N. A.	Δ3,3-D_2-Cys	Δ^{15}N-Cys	$\Delta^{14}N/^{15}N^a$	$\Delta^{63}Cu/^{65}Cu^a$	$\Delta^{32}S/^{34}S^a$	major contribution mode
267.3	−1.3[b]	−0.7	−1.6	−0.3		νCu−N(His)
375.0	−1.8	−1.0	−1.8	−0.1	−1.0	νCu−S + δCβCαN + δCβCαS
386.3	−2.3	−1.4	−2.2	−0.2	−0.3	δCβCαN
395.4	−0.9	−0.2	−0.2	−0.3		δCβCαC(O)
403.8	−3.2	−0.2	−1.5	−0.2	−0.8	δSCβCα
422.0	−1.3	−1.4	−2.4	−0.2	−2.2	νCu−S + δCβCαN + δCβCαS
430.4	−0.4	−0.2	−1.6	−0.7	−2.3	νCu−S
440.2	−1.1	+0.2	−2.0	−1.0	−0.9	
463.5	−0.2	−1.2	−2.2	−0.2		
total shift	−12.8	−6.5	−15.5	−3.2		

[a] Data from ref 8. [b] Estimated uncertainty for all the isotope shifts = ±0.2 cm^{-1}.

imidazole ligand).[22] Consequently the extra 2 cm^{-1} must result from amide exchange of the ligating or of nearby residues.

Within this context of extensive mixing, however, one can see some selectivity in the collected isotope shifts, permitting qualitative assignments (Table 1). Thus the 430 and 440 cm^{-1} peaks exhibit the largest $^{63/65}$Cu isotope shifts, over $^1/_2$ of the total shift for this isotope, and therefore qualify as Cu−S stretching modes. Since, however, there is only one Cu−S bond and since almost half of the total $^{63/65}$Cu isotope shift is distributed over other peaks, it is evident that the 430 and 440 cm^{-1} modes must have important contributions from other coordinates. The Cys-^{15}N shifts are small, but the all-^{15}N shifts are substantial, indicating that the mixing coordinates have major contributions either from the histidine ligands (there are out-of-plane imidazole coordinates with natural frequencies in this region)[23] or from amide groups other than that of the cysteine ligand.

Relatively large Cys-^{15}N shifts are seen for the 375, 386, 422, and 464 cm^{-1} peaks, suggesting important contributions from the cysteine $C_\beta C_\alpha N$ bending coordinate. These bands also show appreciable cysteine $C_\beta D_2$ shifts, as expected. However, the 395 and 404 cm^{-1} bands show large $C_\beta D_2$ but small Cys-^{15}N shifts, suggesting major contributions from other cysteine coordinates, probably $SC_\beta C_\alpha$ and $C_\beta C_\alpha C(O)$ bending.

Interestingly, the most intense peak, at 422 cm^{-1}, has only a small $^{63/65}$Cu shift but substantial shifts for all the cysteine labels and for the all-^{15}N sample. The peaks with large $^{63/65}$Cu shifts, 430 and 440 cm^{-1}, have substantial intensities but are not stronger than the bands at 375, 386, 395, and 404 cm^{-1}, which have small $^{63/65}$Cu shifts. Cu−S stretching has generally been assumed to be the intensity-generating coordinate[5c,9,10] since the Cu−S bond is expected to be directly affected in the charge-transfer excited state. However, this assumption was found not to work very well in the Pcy modeling effort.[11] It is evident that other coordinates of the protein contribute at least as much to the RR intensities as the Cu−S stretch.

3.2. Overtones and Combinations at 500−1000 cm^{-1}, νS−C and Duschinsky Rotation. As noted by Woodruff and co-workers[20] Pcy exhibits RR enhancement of overtone and combination bands of the peaks in the 400 cm^{-1} region (Figure 5). These cluster around an additional band at 762 cm^{-1} which was suggested to be the S−C stretching mode (νS−C, of the bound cysteine).[5a,20] This assignment is confirmed by the large downshift, to 702 cm^{-1}, in the $C_\beta D_2$ sample. The scattering envelope in this region can be understood as arising from overtones and combinations of all seven fundamentals between 375 and 440 cm^{-1}, contributing with comparable intensities.

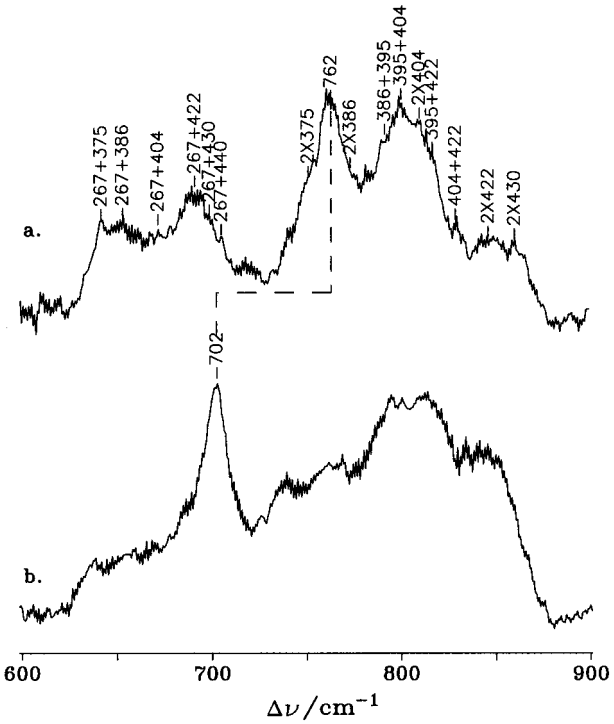

Figure 5. Middle frequency range of RR spectra of Pcy. (a) N. A. Pcy, 647 nm excitation; (b) β-D_2-Cys Pcy, 530 nm excitation.

The intensity is highest in the middle of the envelope, corresponding to the highest density of states. This profuson of combination modes has been interpreted as evidence for Duschinsky rotation of the normal coordinates in the excited state, as a result of a large geometry change.[5c]

Additional evidence of Duschinsky rotation can be observed in the 600−700 cm^{-1} region, where our spectra reveal a set of peaks, whose relative intensities mirror those of the 400 cm^{-1} region peaks (Figure 5). These are combinations of the 267 cm^{-1} mode with all the ∼400 cm^{-1} fundamentals.

3.3. Enhancement of Cysteine and Histidine Internal Modes. It has long been known that the high-frequency region of type 1 Cu protein RR spectra contain additional peaks, which are weak but are nevertheless resonance-enhanced.[20] These peaks are displayed in Figure 6, where the enhancement may be gauged from the very weak peak at 1003 cm^{-1}, which is the strongest Raman peak of phenylalanine.[24] There are seven Phe residues in Pcy, so that unenhanced Raman scattering from the protein is seen to be negligible.

Moreover, all the peaks may now be assigned to internal modes of cysteine and histidine residues, because of the shifts

(22) (a) Chazin, W. J.; Wright, P. E. *J. Mol. Biol*. **1988**, *202*, 623−636. (b) Badsberg, U.; Jørgensen, A. M. M.; Gesmar, H.; Led, J. J.; Hammerstad, J. M.; Jespersen, L.-L.; and Ulstrup, J. *Biochemistry* **1996**, *35*, 7021−7031.

(23) Woodruff, W. H.; Norton, K. A.; Swanson, B. I.; Fry, H. A. *J. Am. Chem. Soc.* **1983**, *105*, 657−658.

(24) Harada, I.; Takeuchi, H. In *Advances in Infrared and Raman Spectroscopy*; Clark, R. J. H., Hester, R. E., Eds.; John Wiley and Sons: New York, 1986, Vol. 12, pp 113−183.

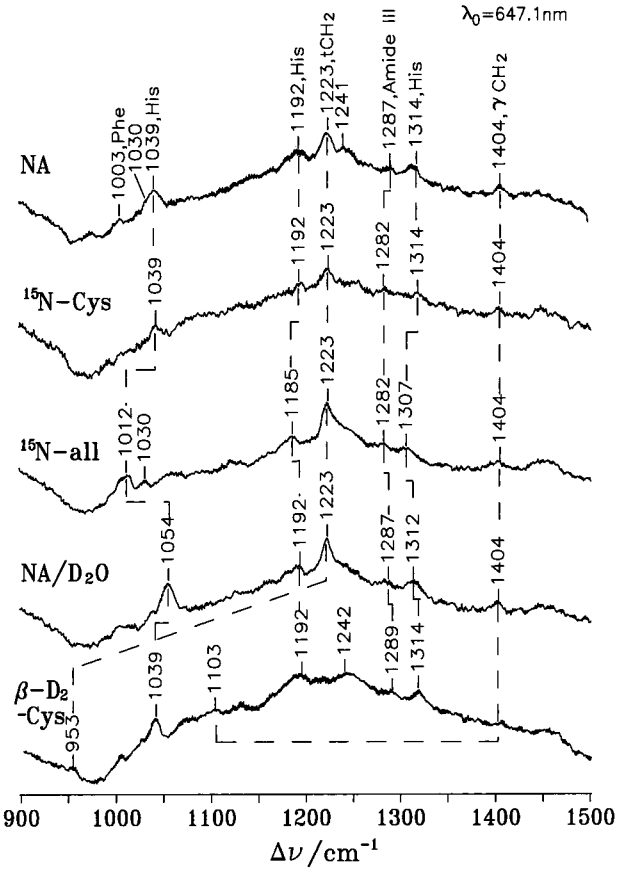

Figure 6. High wavenumber range of the Pcy RR spectra. (a) N.A; (b) ^{15}N-Cys; (c) ^{15}N uniformly labeled; (d) N. A. Pcy in D_2O buffer; (e) β-D_2-Cys labeled.

observed upon isotope labeling (Table 2). The bands at 1122 and 1404 cm^{-1} are twisting and scissors modes of cysteine $C_\beta H_2$ groups, as revealed by the large shifts (to 953 and 1103 cm^{-1}) upon selective deuteration.[25] Also, the 1287 cm^{-1} band arises from the cysteine amide III mode; it shifts appropriately[26] in the ^{15}N-Cys spectrum, and does *not* shift any further in the all-^{15}N spectrum, establishing that the amide III of cysteine has been selected for RR enhancement from among all the other peptide bonds. This frequency is within the amide III frequency range found for β-turn structures of polypeptide,[26c] consistent with the position of Cys84 at the beginning of a β-turn.[2a,7] The selective enhancement of the three cysteine modes is direct evidence for the involvement of cysteine ligand coordinates in the charge-transfer excited state.

The remaining three bands, 1039, 1192, and 1314 cm^{-1}, are all assignable to histidine residues. They shift to lower frequencies in the all-^{15}N spectrum but not in the ^{15}N-Cys spectrum, as expected for imidazole ring modes.[27] (Although a peptide C−C−N skeletal mode is also expected[26] near 1039 cm^{-1}, its ^{15}N shift is much less than the observed 28 cm^{-1}.) Importantly, the 1039 cm^{-1} band shifts *up*, to 1054 cm^{-1}, when the protein is exposed briefly to D_2O, and this shift is reversed upon back-exchange with H_2O. This upshift is a consequence of altered mode composition due to the ring NH/D replacement, which lowers the N−H/D bending frequency below the natural frequency of the ring mode. Since only the His87 NH group, which is exposed to solvent, is exchanged on the time scale of the experiment,[18] enhancement of the 1039 cm^{-1} band is specifically associated with His87; if the second His37 ligand contributed significantly, then a remnant 1039 cm^{-1} band would be seen in the D_2O spectrum since its NH group is not exchanged.[22] Moreover, extended exchange, which produced an added shift in the 267 cm^{-1} Cu−N(His) mode but no further effect on the 1054 cm^{-1} band, confirmed the lack of His37 involvement. It seems likely that the 1192- and 1314-cm^{-1} ring modes are likewise associated with His87.

Why should RR enhancement in the CT absorption band be specific for His87? Figure 1 shows that the His87 imidazole ring is nearly orthogonal (72°) to the CuN_2S plane, while the His37 imidazole lies in this plane. Thus the N π orbital for His87, but not His37, is correctly aligned for overlap with the cysteine S π orbital, and the half-filled orbital on Cu ($d_{x^2-y^2}$), which is the acceptor orbital for the S → Cu CT transitions. To the extent that there is imidazole → Cu π donation in the ground state, the imidazole π bonding will be affected by the CT transition, thus providing a mechanism for RR enhancement of the imidazole ring modes.

3.4. Raman Excitation Profiles. Although enhancement of all RR peaks within the CT absorption band has long been recognized,[5] we find that relative intensities depend on the excitation wavelength within the band envelope. As seen in Figure 7, the 267 cm^{-1} peak steadily gains intensity relative to the ∼400 cm^{-1} peaks as the wavelength is changed from the blue side of the absorption band to the red side even though the overall scattering strength follows the absorption band contour (see the unenhanced 225 cm^{-1} ice band). This effect is quantitated in the excitation profiles (Figure 8). For the group of peaks near 400 cm^{-1} (whose overlapped intensities are integrated for this purpose), the EP maximum is slightly to the blue (590 nm) of the strong 600 nm absorption band, which has been assigned[4] to S π → Cu CT. The EP also displays a shoulder at ∼520 nm, where a weaker S pseudo-σ CT transition has been assigned.[4] Essentially the same profiles are observed (albeit with much lower cross sections) for the 762 cm^{-1} C−S stretching peak, and the 1223 cm^{-1} Cys $C_\beta H_2$ twist peak, both of which arise from cysteine coordinates. However, the EP maximum is shifted to the red of the 600 nm absorption band for the 267 cm^{-1} Cu−N(His) stretching peak (602 nm), and for the 1039 cm^{-1} His87 imidazole ring peak (608 nm). Thus, the RR peaks associated primarily with the His87 ligand have distinctively red-shifted EPs, relative to those associated primarily with the cysteine.

We propose that the 600 nm absorption band actually contains CT transitions from both cysteine and His87. The imidazole ring has two close-lying HOMOs π_1 and π_2.[28] Calculations by Solomon and co-workers[29] place the π_1 energy close to those of the Cu d_{xz} and d_{yz} orbitals; the orbital energy order is d_{xz}, d_{yz} ≈ Hisπ_1 > Cysπ ≫ Hisπ_2. Since the Cu $d_{xz,yz}$ → $d_{z^2-y^2}$ transition has been assigned at 717 nm and since the $d_{x^2-y^2}$ is the acceptor orbital for the CT as well as the d−d transitions, it follows that the imidazole π_1 CT should be somewhat lower in energy than the S π CT transition. The imidazole π_1 CT

(25) (a) Li, H.; Wurrey, C. J.; Thomas, G. J., Jr. *J. Am. Chem. Soc.* **1992**, *114*, 7463−7469. (b) Susi, H.; Byler, D. M.; Gerasimowics, W. V. *J. Mol. Struct.* **1983**, *102*, 63−79.

(26) (a) Krimm, S. In *Vibrational Spectra and Structure*; Durig, J. R., Ed.; Elsevier: New York, 1972; Vol. 16, pp 1−72. (b) Suzuki, S.; Iwashita, Y.; Shimanouchi, T.; Tsuboi, M. *Biopolymers* **1966**, *4*, 337−350. (c) Tu, A. T. In *Spectroscopy of Biological Systems*; Clark, R. J. H., Hester, R. E., Eds.; John Wiley & Sons Ltd.: New York, 1986; pp 47−112.

(27) (a) Caswell, D. S.; Spiro, T. G. *J. Am. Chem. Soc.* **1986**, *108*, 6470−6477,. (b) Tasumi, M.; Harada, I.; Takamatsu, T.; Takahashi, S. *J. Raman Spectr*. **1982**, *12*, 149−151. (c) Ashikawa, I.; Ttoh, K. *Biopolymers* **1979,** *18*, 1859−1876.

(28) Del Bene, J.; Jaffé, H. H. *J. Chem. Phys.* **1968**, *48*, 4050−4055.

(29) Guckert, J. A.; Lowery, M. D.; Solomon, E. I. *J. Am. Chem. Soc.* **1995**, *117*, 2817−2844.

Table 2. RR Bands of Plastocyanin between 950 cm^{-1} and 1450 cm^{-1}

N. A.	$\Delta^{15}N$	$\Delta^{15}N$-Cys	$\Delta\beta$-D_2-Cys	ΔN. A. in D_2O	assignment	analogous modes in *L*-Cys[a] and $Cu(Im)_4^{2+}$ [b]
1003					Phe ring breathing (F1)	
1039	−28			+15	His87 symmetric N−C−N stretch + N−H bending	1081
1192	−7				His ring mode	1191
1122			−169		Cys84 CH_2 twist	1273
1286	−4	−4	+3		amide III of Cys84	
1314	−7			−2	His ring mode	1332
1404			−331		Cys84 CH_2 scissor	1427

[a] Reference 25. [b] Reference 27.

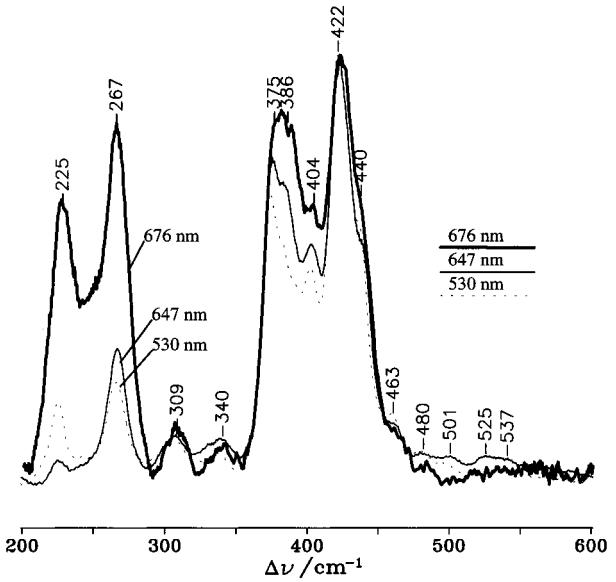

Figure 7. Low wavenumber range of N. A. Pcy RR spectra excited at different wavelengths. Spectra were normalized to the peak at 422 cm^{-1}. (a) 676 nm; (b) 647 nm; (c) 530 nm. The same protein droplet was used for all of the spectra. Protein was dissolved in 20 mM pH 6.0 bis-Tris buffer with 150 mM NaCl. The spectral slit was kept at 3 cm^{-1} for all three spectra.

transition was originally assigned to a weak 480 nm absorption band,[4a,30,31] but in view of the more recent calculations,[29] this higher-energy transition should instead involve CT from the deeper-lying π_2 transition.[29,32] The closely spaced transitions in the 600 nm absorption band, suggested by the RR EPs, could then arise from CT transitions to Cu involving a combination of S π and imidazole π_1 orbitals. Recent calculations by Solomon and co-workers[31] indeed predict a 7% contribution from the imidazole to the mainly S π CT transition. Since the Cu−S bond is more covalent than the Cu−N (imidazole) bond and since the π_1 orbital has a smaller contribution from the N than the C atoms on imidazole,[29] the overall contribution of the π_1 orbital to the 600 nm absorption strength is undoubtedly small. Nevertheless, the distinguishability of the Cys-based and His-based EPs does support the view that imidazole is involved in the absorption and that there are two closely spaced CT transitions with contributions from both Cys π and His π_1 orbitals. This inference may affect the quantitative modeling of the EP's[13] since the contributions from the two transitions are expected to interfere.

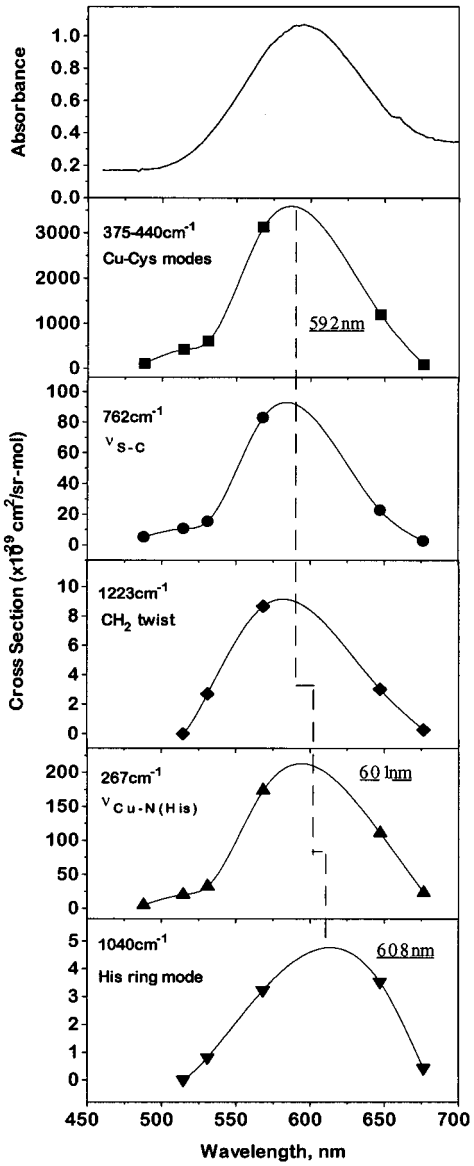

Figure 8. Excitation profiles for the indicated RR peaks, compared with the absorption spectrum (top). Intensities were obtained from band areas after background subtraction and baseline correction. Uncertainties associated with these corrections are estimated to be less than 15%, even for the weakest bands, and are usually much less. The intensities were referenced to the ice or sulfate peaks, as described in the Experimental Section. The profile maxima were obtained by fitting a Gaussian function to the data points (which are connected by spline lines in the figure).

4. Discussion

The ET mechanisms of Pcy have been investigated extensively from both experimental[1a,33] and theoretical[34] perspectives. Two ET pathways have been established, one through the His87

(30) Gewirth, A. A.; Solomon, E. I. *J. Am. Chem. Soc.* **1988**, *110*, 3811−3819.
(31) LaCroix, B.; Shadle, S. E.; Wang, Y.; Averill, B. A.; Hedman, B.; Hudgson, K. O.; Soloman, E. I. *J. Am. Chem. Soc.* **1996**, *118*, 7755−7768.
(32) Penfield, K. W.; Gay, R. R.; Himmelwright, R. S.; Eickman, N. C.; Norris, V. A.; Freeman, H. C.; Solomon, E. I. *J. Am. Chem. Soc.* **1981**, *103*, 4382−4388.

ligand and the other through the Cys84 ligand. The His87 imidazole ring is exposed to solvent and provides a short route (∼6 Å) for the transferring electron; however, the Cys84 ligand is buried, and the electron travels a long distance (∼13 Å) via the remote Tyr83 side chain, which is solvent exposed (Figure 1). This remote site has been established by chromium affinity labeling[35] and Tyr83 mutation[36] to be the route for reduction of Pcy by its biological partner, cyt b_6f, while His87 is the route for oxidation by photosystem I, as shown by mutation[37] and photolysis studies.[38]

The CT transitions of Pcy are closely associated with the ET mechanism since the resulting electronic configuration has a hole on the Cys84 (Cu^{I}-$S^{\bullet+}$) and/or His87 (Cu^{I}-$ImH^{\bullet+}$) ligands. In fact these represent the dominant virtual states in the superexchange model of the ET process.[39] Consequently the RR enhancement pattern is directly relevant to the elucidation of the ET mechanism, as emphasized recently by Loppnow and co-workers[13] and by Scherer and co-workers.[40] The Franck−Condon factors that determine the scattering cross sections are also those involved in the hole-transfer integrals. Thus, the identification of resonance-enhanced internal modes of the Cys84 and His87 ligands provide direct evidence for electronic coupling along both the remote and adjacent ET pathways in Pcy. When charge is transferred to Cu^{II}, the resulting hole extends to the imidazole ring on one side and to the cysteine side chain and its amide bond on the other.

Redox reactions of Pcy with small molecules have similar rates through the remote and adjacent sites, despite the large difference in the ET distance.[34] Thus, the remote site has a larger electronic coupling factor. This long-range electronic coupling is undoubtedly faciliatated by the strong S → Cu donation and by the coplanar CuSCCN framework (Figure 1). This coplanar arrangement provides optimum overlap of orbitals for either electron or hole transfer.

The coplanarity also helps explain the complex nature of the low-frequency RR modes.[5b,41] RR enhancement by CT electronic transitions is normally dominated by metal−ligand stretching modes, with only secondary involvement of ligand coordinates.[42] But in all type 1 Cu proteins, Cu−S stretching is heavily mixed with internal ligand modes. Strikingly, this mixing is preserved, although its nature is altered, even when the Cu−S stretching frequency is lowered via bonding changes resulting from mutagenesis.[43] As the Cu−S bond is weakened, intensity is shifted to lower frequency RR bands, but the spectra retain multiple peaks. Thus the Cu−S coordinate appears to select different ligand coordinates for mixing as its frequency is brought into coincidence with theirs. This unusual behavior must reflect the multiple coupling opportunities afforded by the coplanarity of the extensive atomic framework connected to the ligating S atom. Thus, this coplanar framework, which may have evolved to maximize the ET rate from the remote site, is also responsible for the complex RR spectral pattern.

The present work emphasizes that orbital alignment extends to the adjacent His87 site as well. The orientation of the imidazole ring permits overlap of its orbital with the Cys84 π orbital through the intervening Cu $d_{x^2-y^2}$ orbital. Moreover, the ligand π orbitals have similar energies, permitting mixing of the CT transitions. This mixing is evident in the enhancement of imidazole ring modes, which are specifically associated with His87 and the shifted excitation profiles for imidazole vs cysteine vibrations. The His87 orientation may also explain the unusual mixing of the Cu−N(His) stretching coordinate with the cysteine coordinates, as evidenced by the isotope sensitivity of the 267 cm^{-1} band.

Acknowledgment. We thank Professor Michael Hecht and Dr. Joel Ybe for generous assistance with Pcy expression. This work was supported by NIH Grant GM13498 from the National Institute of General Medical Science.

JA974377P

(33) Farver, O.; Pecht, I. *Coord. Chem. Rev.* **1989**, *94*, 17−45.
(34) (a) Lowery, M. D.; Guckert, J. A.; Gebhard, M. S.; Solomon, E. I. *J. Am. Chem. Soc*. **1993**, *115*, 3012−3013. (b) Beratan, D. N.; Betts, J. N.; Onuchic, J. N. *Science* **1991**, *252*, 1285−1288.
(35) Farver, O.; Pecht, I. *Proc. Natl. Acad. Sci. U.S.A.* **1981**, *78*, 4190−4193.
(36) He, S.; Modi, S.; Bendall, D. S.; Gray, J. C. *EMBO J.* **1991**, *10*, 4011−4016.
(37) Sigfridsson, K.; Young, S.; Hansson, Ö. *Biochem*istry **1996**, *35*, 1249−1257.
(38) Qin, L.; Kostic, N. M. *Biochemistry* **1996**, *35*, 3379−3386.
(39) Newton, M. D. *Chem. Rev.* **1991**, *91*, 767−792.
(40) Ungar, L. W.; Scherer, N. F.; Voth, G. A. *Biophys. J.* **1997**, *72*, 5−17.
(41) Han, J.; Adman, E. T.; Beppu, T.; Codd, R.; Freeman, H. C.; Huq, L.; Loehr, T. M.; Sanders-Loehr, J. *Biochemistry* **1991**, *30*, 10904−10913.
(42) Qiu, D.; Kilpatrick, L.; Kitajima, N.; Spiro, T. G. *J. Am. Chem. Soc.* **1994**, *116*, 2585−2590.
(43) Andrew, C. R.; Anders-Loehr, J. *Acc. Chem. Res.* **1996**, *29*, 365−372.